Journal of Biomechanics 85 (2019) 198–203

Contents lists available at ScienceDirect

Journal of Biomechanics

journal homepage: www.elsevier.com/locate/jbiomech
www.JBiomech.com

Short communication

Site- and sex-differences in morphological and mechanical properties of the plantar fascia: A supersonic shear imaging study

Hiroto Shiotani [a], Ryo Yamashita [b], Tomohiro Mizokuchi [b], Munekazu Naito [c], Yasuo Kawakami [d,*]

[a] Graduate School of Sport Sciences, Waseda University, Saitama, Japan
[b] School of Sport Sciences, Waseda University, Saitama, Japan
[c] Department of Anatomy, Aichi Medical University, Aichi, Japan
[d] Faculty of Sport Sciences, Waseda University, Saitama, Japan

ARTICLE INFO

Article history:
Accepted 5 January 2019

Keywords:
Plantar aponeurosis
Elasticity
Thickness
Site-dependence
Shear wave elastography

ABSTRACT

The purpose of this study was to investigate the site- and sex-differences in the morphological and mechanical properties of the plantar fascia (PF) in humans. The thickness and shear wave velocity (SWV) of PF at five different sites between the medial calcaneal tubercle and the second toe were measured for 40 healthy young participants (20 males and 20 females) using supersonic shear imaging (SSI). The thickness and SWV measurements were highly repeatable (ICC $\geq$ 0.93). The proximal sites of PF around the calcaneal attachment were significantly thicker and stiffer (higher SWV values) than the middle and distal sites ($p < 0.05$). In addition, females had significantly thinner PF in proximal and middle sites than males, while being significantly stiffer in regardless of the sites, compared with males ($p < 0.05$). The results of the present study partly support previous findings on the site- and sex-differences in PF morphology, and further reveal inhomogeneity and sex-specificity of PF stiffness. The present study widely opens the possibility of evaluating PF functions *in vivo*.

1. Introduction

The plantar fascia (PF) stretches from the medial calcaneal tubercle to the proximal phalanges of five toes, and is known as an anatomical constituent of the arch of the foot (Hicks, 1954; Stecco et al., 2013). The PF is categorized as the passive linking fascia, which plays an important role in passive force transmission (Kumka and Bonar, 2012; Stecco et al., 2013). It has been demonstrated that PF behaves visco-elastically under tension (Ker et al., 1987; Pavan et al., 2011), thereby stabilizing the medial longitudinal arch of the foot (Caravaggi et al., 2010; Huang et al., 1993) and contributing myofascial (with toe flexor muscles) and myotendinous (with the Achilles tendon) force transmission from the hind- to forefoot during exercises (Carlson et al., 2000; Cheung et al., 2006; Erdemir et al., 2004; Hamel et al., 2001; Hanna and Schmitt, 2011). Most of these notions have been derived from cadaveric studies. It has however been suggested that the mechanical properties of the cadavers' soft tissues differ from those of the tissues *in vivo*, through the preservation and fixation procedures (Ling et al., 2016; Wilke et al., 2011).

During daily exercises, PF is mechanically stretched, thus the morphological and mechanical properties of PF may adapt to such stress accumulation. A previous simulation study using a three-dimensional finite element foot model suggested that the distribution of the tension and peak stress along PF is site-specific (Chen et al., 2015). This result has partly been substantiated through *in vivo* studies on PF morphology (e.g., thickness measurement by B-mode ultrasonography) showing site-specific differences in PF thickness (Crofts et al., 2014), and a common site of plantar fasciitis being at the proximity to the calcaneal attachment (Gibbon and Long, 1999). Furthermore, PF thickness at the calcaneal attachment is known to be thinner in females than in males (Huerta and Garcia, 2007). The females' medial longitudinal arches are more deformable with weight bearing than those of males (Fukano and Fukubayashi, 2012), and females have greater incidence rates of the plantar fasciitis than males (Scher et al., 2009; Werner et al., 2010). These pieces of evidence suggest the site- and sex-differences of the mechanical properties of PF, which has not been clarified through *in vivo* measurements.

The ultrasound shear wave elastography is a relatively new technique that quantitatively evaluates soft tissue stiffness. It measures the velocity of mechanical waves in shear direction propagating within the soft tissues generated by acoustic radiation force pulse signals emitted from the ultrasound transducer (Bercoff

* Corresponding author at: Faculty of Sport Sciences, Waseda University, 2-579-15 Mikajima, Tokorozawa, Saitama 359-1192 Japan.
E-mail address: ykawa@waseda.jp (Y. Kawakami).

https://doi.org/10.1016/j.jbiomech.2019.01.014
0021-9290/

et al., 2004). The shear wave velocity (SWV) directly reflects the Young's modulus of the soft tissue (Ates et al., 2018; Eby et al., 2013), therefore it can be a measure of the stiffness of the soft tissues. Among existing elastography techniques, supersonic shear imaging (SSI) has several advantages over others with respect to higher reproducibility, range of measurement values and spatial and time resolution (Lima et al., 2017). There is only one attempt that used SSI to evaluate stiffness of PF *in vivo* (Zhang et al., 2014), however, the site- and sex-differences in PF stiffness has not been investigated. In this study, we used SSI to test our hypothesis that both the morphological and mechanical properties of PF are site- and sex-specific.

Table 1
Physical characteristics and the foot dimensions of the participants.

	Males	Females	*p* value
Age (years)	22.8 ± 2.0	22.2 ± 1.8	0.41
Height (m)	1.71 ± 0.05	1.61 ± 0.05	<0.01*
Body mass (kg)	60.3 ± 7.5	54.1 ± 6.4	<0.01*
BMI (kg/m^2)	20.6 ± 2.3	21.0 ± 2.6	0.51
Foot length (mm)	249.4 ± 8.8	233.2 ± 6.9	<0.01*
Ball width (mm)	98.1 ± 3.6	93.2 ± 4.3	<0.01*
Heel width (mm)	62.8 ± 3.8	59.8 ± 3.7	<0.01*
Navicular height (mm)	43.0 ± 5.6	35.9 ± 6.3	<0.01*
Arch ratio (%)	17.1 ± 2.4	15.4 ± 2.5	<0.01*

Values are mean ± SDs. The foot length, ball width, heel width and navicular height were measured using three-dimensional foot scanner (JMS-2100CU, Dream GP, Osaka, Japan) with the same protocol used in a previous study (Fukano and Iso, 2016). The arch ratio was calculated as the percent of the navicular height over the foot length. *Significant difference between males and females tested by independent t-tests ($p < 0.01$). BMI – Body mass index.

2. Methods

2.1. Testing procedures

Forty participants (20 males and 20 females; age 22.5 ± 1.9 years, height 1.66 ± 0.07 m, and body mass 57.2 ± 7.5 kg; means ± standard deviations) with no history of foot or ankle injuries, or continuous exercise habits in the 12 months prior to the measurement, were recruited. Participants were not allowed to perform any strenuous exercises for at least 24 h before the measurement. Physical characteristics and foot dimensions of the participants are shown in Table 1. This study was approved by

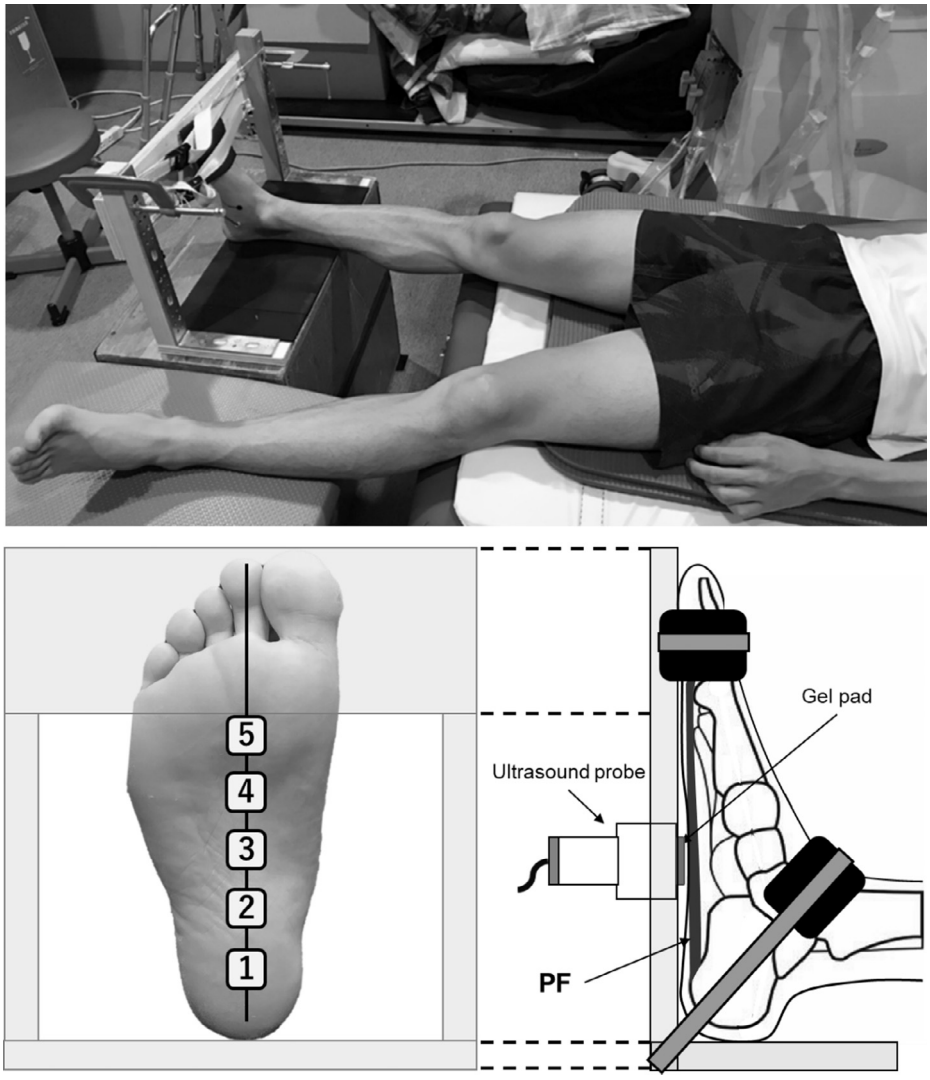

Fig. 1. Experimental setup for SSI measurement. The ankle and toe digits were secured to a custom-made fixture at the neutral positions. The scanning of PF was performed at five different sites along the longitudinal line between the medial calcaneal tubercle and the second toe. The long axis of the transducer was placed along this longitudinal line. All data collections were carried out in the controlled condition at the room temperature 25 ± 1 °C to minimize the temperature-related changes in mechanical properties of the soft tissues (Akagi and Takahashi, 2013; Kawakami et al., 2008; Strickler et al., 1990).

the Institutional Human Research Ethics Committee and was carried out in accordance with the Declaration of Helsinki. Written informed consent was obtained from all participants beforehand.

Participants were requested to rest in a supine position on an examination bed with the knee fully extended and the feet off the edge of the bed, and their right/left foot and toe digits were secured to a custom-made fixture in random order (Fig. 1). The ankle joint and toe digits were kept at the neutral positions, which was confirmed with a handheld goniometer. Care was taken to avoid any mechanical pressure acting on the surface of the sole of the foot. The SSI measurement was performed using an Aixplorer ultrasound scanner (version 6.4, Supersonic Imagine, Aix-en-Provence, France) with a linear array transducer (SL 15-4, Supersonic Imagine, Aix-en-Provence, France) to measure PF thickness and SWV of the bilateral feet. The scanner was set at the musculoskeletal (MSK) preset and penetration mode with medium persistence and high spatial smoothing (9/9). All measurements were conducted by the same examiner, with the transducer manually operated. The scanning head of the transducer was coated with transmission gel and an acoustic standoff pad (Gelpad for StatUS^{TM}, Enraf-Nonius, Rotterdam, Netherland) was used to avoid applying excessive compression on the skin surface. The scanning of PF was performed in a longitudinal direction at five different sites along the longitudinal line between the medial calcaneal tubercle and the second toe (Figs. 1 and 2). This longitudinal line and the locations of the transducer were marked on the skin surface using a waterproof marker. At each site, ultrasound B-mode images and shear wave data were collected for 5–7 s with a system operating at 12 Hz (i.e., the default sampling rate of SSI measurement of the current version of the ultrasound scanner).

After the data collection, PF was visually identified in the ultrasound images, and the region of interest (ROI) was determined to cover the fascial boundaries of PF (Fig. 2). Three images separated by 12 frames were picked up and analyzed for PF thickness and SWV, then the three values were averaged to obtain the representative values. It should be mentioned that strictly, SWV measurement of PF included the surface acoustic wave signals from the thin layer of the soft tissues (Saavedra et al., 2017), but in the present study we defined our measurements as SWV.

2.2. Statistical analysis

All data are presented as means ± standard deviations (SDs) unless otherwise indicated. The reliability of the PF thickness and SWV was determined across the three consecutive measurements at each site. The intraclass correlation coefficient (ICC), standard error of the mean (SEM), and coefficient of variation (CV) were calculated (Hopkins, 2000). A two-way analysis of variance (ANOVA) (sites × sex) with repeated measures were performed to compare PF thickness and SWV among five measurement sites and between males and females. If a significant main effect and/or interaction was found, one-way ANOVA with a Bonferroni correction for sites and independent *t*-tests for sex were performed.

Univariate linear regression was used to find the best fit of SWV to thickness both in males and females for overall and individual measurement sites. For all statistical analyses, the level of significance was set at $p < 0.05$. Statistical analyses were performed using an SPSS software (SPSS Statistics 24, IBM, USA).

3. Results

The repeatability of PF thickness and SWV was excellent for every measurement site, with ICC values ≥0.93 (Table 2). The PF thickness was highest at Site 1 and significantly smaller distally in both sex (Fig. 3a). There were significant differences among all measurement sites both in males and females ($p < 0.001$ and $p < 0.001$, Fig. 3a). Males had significantly thicker PF than females at Site 1–3 (Site 1: $p < 0.001$, Site 2: $p = 0.002$, Site 3: and $p = 0.045$, Fig. 3a).

The SWV values at Site 1 were significantly higher in Site 3–5 than that of males (Site 3: $p < 0.001$, Site 4: $p < 0.001$, and Site 5: $p < 0.001$) and females (Site 3: $p < 0.001$, Site 4: $p < 0.001$, and Site

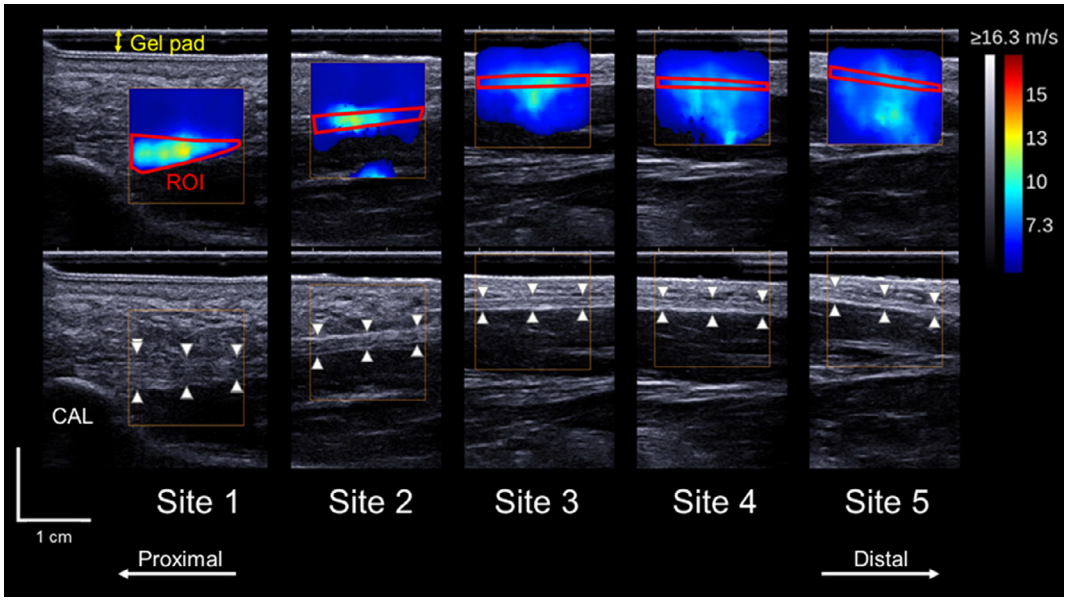

Fig. 2. Representative example of ultrasound images of PF. An acoustic standoff pad was used for all measurements. B-mode and shear wave elastography-mode images were obtained at each measurement site. Site 1 – PF at the calcaneal (CAL) attachment, Site 2 – at the midpoint of Site 1 and 3, Site 3 – at the level of the navicular tubercle, Site 4 – at the midpoint of Site 3 and 5, and Site 5 – proximity to the second metatarsal head. PF was visually identified, and thickness and SWV were measured. PF thickness was defined as the distance between superficial and deep fascial boundaries of PF. The SWV was obtained the mean values within ROI (drawn in red for clarity) which manually defined using a measurement tools (Q-Box^{TM} Trace) with avoiding the saturation (values that reached the maximal measurable SWV) and the rejection (without measurable SWV values) in shear wave elastography-mode images.

Table 2
Repeatability of PF thickness and shear wave velocity for each measurement site.

		Site 1	Site 2	Site 3	Site 4	Site 5
Thickness	ICC (3.1)	0.97	0.96	0.97	0.96	0.93
	SEM (mm)	0.05	0.04	0.03	0.02	0.02
	CV (%)	2.49	2.59	2.30	2.99	3.46
Shear wave velocity	ICC (3.1)	0.94	0.96	0.96	0.98	0.97
	SEM (m/s)	0.27	0.24	0.18	0.20	0.20
	CV (%)	3.88	3.58	4.02	3.44	3.76

ICC – Intraclass correlation coefficient; SEM – Standard error of the mean; CV – Coefficient of variation.

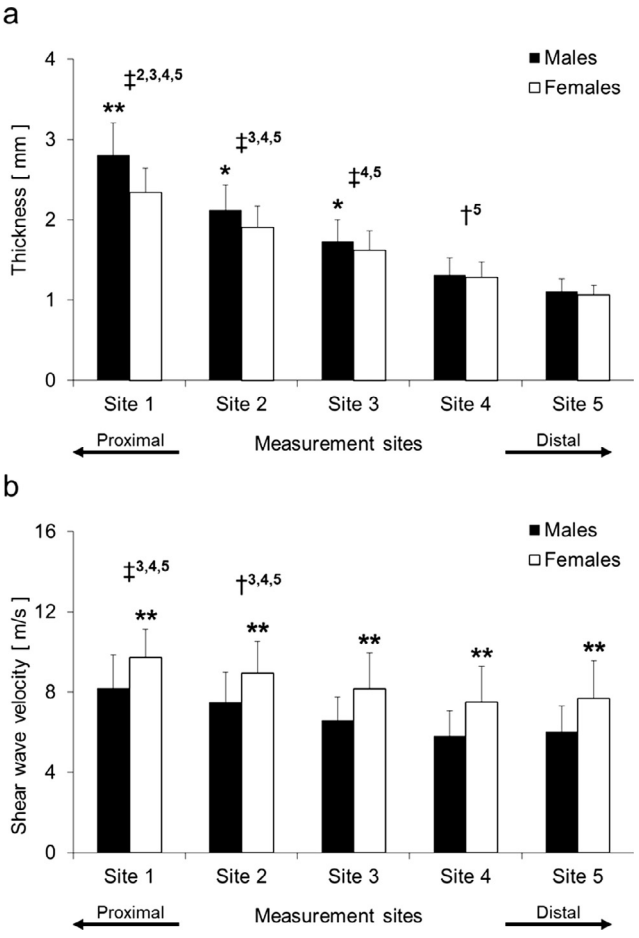

Fig. 3. The site- and sex-differences in PF thicknesses (a) and shear wave velocities (b) for each measurement site. *Significant difference between males and females (*$p < 0.05$, **$p < 0.001$). †Significant difference between sites ($^{\dagger}p < 0.05$, $^{\ddagger}p < 0.001$).

5: $p < 0.001$, Fig. 3b). A similar result was obtained for Site 2 both in males (Site 2 vs. Site 3: $p = 0.026$, Site 4: $p < 0.001$, and Site 5: $p < 0.001$) and females (Site 2 vs. Site 3: $p = 0.019$, Site 4: $p < 0.001$, and Site 5: $p < 0.001$, Fig. 3b). At all measurement sites, females showed significantly higher SWV values than males ($p < 0.001$, Fig. 3b).

There were moderate correlations between SWV and thickness of PF in overall measurement sites both in males and females (males: $r = 0.49$, $p < 0.001$, females: $r = 0.41$, $p < 0.001$). The correlations between SWV and thickness values at individual measurement sites were not significant ($p > 0.05$, Fig. 4).

4. Discussion

The PF thickness and SWV were greater in the proximal compared with the middle and distal sites. Furthermore, females showed higher SWV values even though their PF thicknesses were thinner than males. These findings partly support previous studies on the site- and sex-differences of PF thickness (Crofts et al., 2014; Huerta and Garcia, 2007), and further reveal the inhomogeneity and sex-specificity of PF stiffness.

The SSI measurements of PF afforded high repeatability for both thickness and SWV (Table 2). The results in the site- and sex-differences in PF thickness were consistent with the previous studies using ultrasonography (Crofts et al., 2014; Huerta and Garcia, 2007). Besides, PF thickness at Site 1 was consistent with the standard value of the thickness at the calcaneal attachment (i.e., approximately 2–4 mm) among the young healthy population using ultrasonography (Gibbon and Long, 1999). In the present study, SWV was reported instead of the Young's modulus or shear elastic modulus. Zhang et al. (2014) reported the value of PF stiffness as the Young's modulus, which is converted from SWV based on the assumption of tissue isotropy using the following equation:

$$V_s = \sqrt{\frac{E}{2\rho(1+\mu)}} \quad (1)$$

where V_s is SWV, E is the Young's modulus, ρ is the tissue density (1000 kg/m^3), and μ is the Poisson's ratio (Bercoff et al., 2004). However, this assumption does not hold for PF since it is known as the anisotropic tissue (Moraes do Carmo et al., 2008; Stecco et al., 2013). Consequently, we chose to report the value of PF stiffness as SWV according to previous studies (Aubry et al., 2013; DeWall et al., 2014). Based on the collagen fibers orientation of PF, a transversally isotropic scheme was adopted for PF in a constitutive modeling study (Pavan et al., 2014), but it has never been investigated *in vivo*. Thus, further investigation including measurement on the morphological and mechanical properties of PF in the transverse direction would be necessary for the better understanding of the nature of PF. However, the majority of mechanical stress and strain during exercise could have been applied on PF in the longitudinal direction. Therefore, the present study will provide the important findings including the site- and sex-differences in PF.

Thicker and stiffer PF in the proximity of its length suggests strong and stable anchorage of PF onto the calcaneus. Previous studies reported sizable plantar pressure vertically on the rearfoot during movements (Arnold et al., 2010; Hills et al., 2001). Another study demonstrated that the tension and peak stress along PF during the late stance phase of gait were concentrated on the proximal portion of PF near the medial calcaneus tubercle (Chen et al., 2015). The site-specificity of the morphological and mechanical properties of PF may reflect the adaptation to such site-specific stress accumulation during daily exercises. Moreover, PF plays an important role in myofascial and myotendinous force transmission from hind- to the forefoot (Carlson et al., 2000; Cheung et al., 2006; Erdemir et al., 2004; Hamel et al., 2001). The PF forms compartments with several toe flexor muscles and vertical fascial septae in the hind- and midfoot, but not in the forefoot (Ling and Kumar, 2008). In addition, PF is connected with the paratenon of the Achilles tendon on the calcaneus (Stecco et al., 2013). These

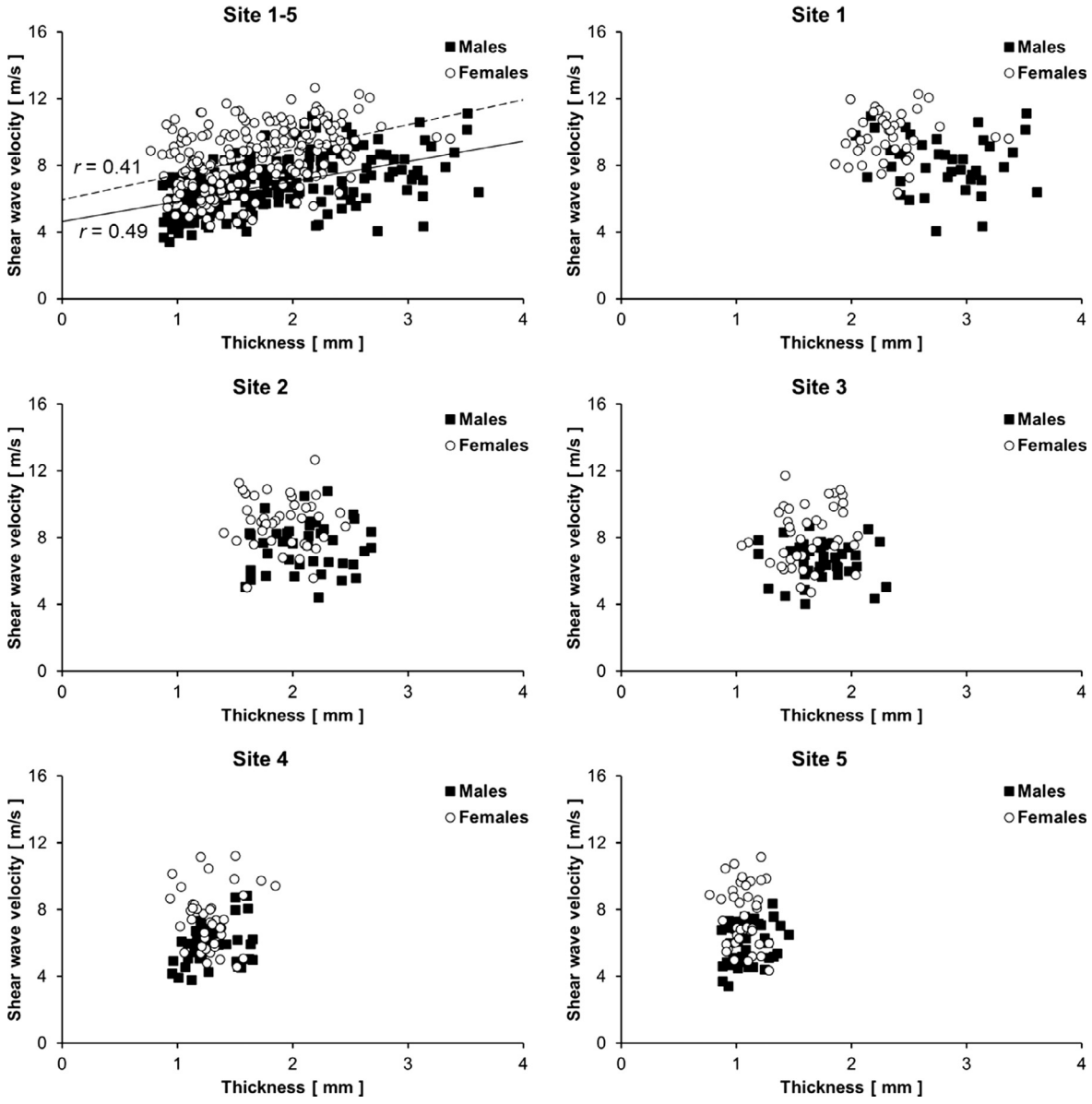

Fig. 4. The relationships between the shear wave velocities and thicknesses of PF in overall and individual measurement sites. In Site1 (proximal) – Site 5 (distal), regression lines are also shown with correlation coefficients in males (bold line) and females (dotted line).

anatomical observations suggest that the myofascial and myotendinous force transmission may occur at the proximal and middle sites of PF. The site-specificity of the morphological and mechanical properties of PF may provide benefits for the fascial force transmission mechanisms.

Thinner but stiffer PF in females is a novel but unexpected finding. The females had smaller foot length, ball, and heel widths (Table 1), thus PF might have been not only thinner, but also shorter and narrower than in males (i.e., PF might have been smaller in females). The larger deformability of a female's longitudinal foot arch may induce greater tensile stress on females' smaller PF during daily exercises. The intrinsic and extrinsic muscles of the foot can also contribute to supporting the arch during dynamic physical activities (Thordarson et al., 1995; Zelik et al., 2015), but females have lower toe flexor muscles' strength than males (Uritani et al., 2014). Considering the fact that females have greater incidence rates of the plantar fasciitis than males (Scher et al., 2009; Werner et al., 2010), there is a possibility that females' PF can be exposed to greater mechanical stress than males. It is therefore suggested that the stiffer PF in females may be a result of compensation for their anatomical and mechanical features.

A moderate correlation between SWV and thickness both in males and females for the overall measurement sites may reflect site-differences since there were no significant correlations between the two parameters in individual measurement sites (Fig. 4). As long as the author's knowledge can reach, this is the first study to examine the relationship between the morphological and mechanical properties of PF measured by using SSI. The results are consistent with previous studies that found only weak correlation between the thickness and SWV of the Achilles tendon (Aubry et al., 2013; DeWall et al., 2014), suggesting that PF thickness is not a primary factor in its stiffness. The B-mode ultrasonography has been clinically used for diagnosing PF abnormality (Draghi et al., 2016), and our observations suggest that SSI can further help evaluating PF status as well as tendons (Aubry et al., 2015; Coombes et al., 2018). The present study widely opens the possibility of evaluating the morphological and mechanical properties of PF *in vivo*, in biomechanical and clinical studies.

In conclusion, we revealed the site- and sex-dependent differences in PF thickness and stiffness. The SWV was higher at the proximal sites, and it was higher in females than males. These differences may reflect the site- and sex-dependence of the mechanical stress on PF during daily exercise.

Conflict of interest

The authors have no conflict of interest.

Acknowledgements

This work was supported by Japan Society for the Promotion of Science KAKENHI Grant Number 16H01870 (Grant-in-Aid for Scientific Research (A)).

References

Akagi, R., Takahashi, H., 2013. Acute effect of static stretching on hardness of the gastrocnemius muscle. Med. Sci. Sports Exerc. 45, 1348–1354.
Arnold, J.B., Causby, R., Pod, G.D., Jones, S., 2010. The impact of increasing body mass on peak and mean plantar pressure in asymptomatic adult subjects during walking. Diabet. Foot Ankle 1, 5518.
Ates, F., Andrade, R.J., Freitas, S.R., Hug, F., Lacourpaille, L., Gross, R., Yucesoy, C.A., Nordez, A., 2018. Passive stiffness of monoarticular lower leg muscles is influenced by knee joint angle. Eur. J. Appl. Physiol. 118, 585–593.
Aubry, S., Nueffer, J.P., Tanter, M., Becce, F., Vidal, C., Michel, F., 2015. Viscoelasticity in Achilles tendonopathy: quantitative assessment by using real-time shear-wave elastography. Radiology 274, 821–829.
Aubry, S., Risson, J.R., Kastler, A., Barbier-Brion, B., Siliman, G., Runge, M., Kastler, B., 2013. Biomechanical properties of the calcaneal tendon in vivo assessed by transient shear wave elastography. Skeletal Radiol. 42, 1143–1150.
Bercoff, J., Tanter, M., Fink, M., 2004. Supersonic shear imaging: a new technique for soft tissue elasticity mapping. IEEE Trans. Ultrason. Ferroelectr. Freq. Control 51, 396–409.
Caravaggi, P., Pataky, T., Gunther, M., Savage, R., Crompton, R., 2010. Dynamics of longitudinal arch support in relation to walking speed: contribution of the plantar aponeurosis. J. Anat. 217, 254–261.
Carlson, R.E., Fleming, L.L., Hutton, W.C., 2000. The biomechanical relationship between the tendoachilles, plantar fascia and metatarsophalangeal joint dorsiflexion angle. Foot Ankle Int. 21, 18–25.
Chen, Y.N., Chang, C.W., Li, C.T., Chang, C.H., Lin, C.F., 2015. Finite element analysis of plantar fascia during walking: a quasi-static simulation. Foot Ankle Int. 36, 90–97.
Cheung, J.T., Zhang, M., An, K.N., 2006. Effect of Achilles tendon loading on plantar fascia tension in the standing foot. Clin. Biomech. (Bristol, Avon) 21, 194–203.
Coombes, B.K., Tucker, K., Vicenzino, B., Vuvan, V., Mellor, R., Heales, L., Nordez, A., Hug, F., 2018. Achilles and patellar tendinopathy display opposite changes in elastic properties: a shear wave elastography study. Scand. J. Med. Sci. Sports 28, 1201–1208.
Crofts, G., Angin, S., Mickle, K.J., Hill, S., Nester, C.J., 2014. Reliability of ultrasound for measurement of selected foot structures. Gait Post. 39, 35–39.
DeWall, R.J., Slane, L.C., Lee, K.S., Thelen, D.G., 2014. Spatial variations in Achilles tendon shear wave speed. J. Biomech. 47, 2685–2692.
Draghi, F., Gitto, S., Bortolotto, C., Draghi, A.G., Ori Belometti, G., 2016. Imaging of plantar fascia disorders: findings on plain radiography, ultrasound and magnetic resonance imaging. Insights Imag. 8, 69–78.
Eby, S.F., Song, P., Chen, S., Chen, Q., Greenleaf, J.F., An, K.N., 2013. Validation of shear wave elastography in skeletal muscle. J. Biomech. 46, 2381–2387.
Erdemir, A., Hamel, A.J., Fauth, A.R., Piazza, S.J., Sharkey, N.A., 2004. Dynamic loading of the plantar aponeurosis in walking. J. Bone Joint Surg. Am. 86, 546–552.
Fukano, M., Fukubayashi, T., 2012. Gender-based differences in the functional deformation of the foot longitudinal arch. Foot 22, 6–9.
Fukano, M., Iso, S., 2016. Changes in foot shape after long-distance running. J. Funct. Morphol. Kinesiol. 1, 30–38.
Gibbon, W.W., Long, G., 1999. Ultrasound of the plantar aponeurosis (fascia). Skeletal Radiol. 28, 21–26.
Hamel, A.J., Donahue, S.W., Sharkey, N.A., 2001. Contributions of active and passive toe flexion to forefoot loading. Clin. Orthop. Relat. Res., 326–334
Hanna, J.B., Schmitt, D., 2011. Comparative triceps surae morphology in primates: a review. Anat. Res. Int. 2011, 191509.
Hicks, J.H., 1954. The mechanics of the foot. II. The plantar aponeurosis and the arch. J. Anat. 88, 25–30.
Hills, A.P., Henning, E.M., McDonald, M., Bar-Or, O., 2001. Plantar pressure differences between obese and non-obese adults: a biomechanical analysis. Int. J. Obes. Relat. Metab. Discord. 25, 1674–1679.
Hopkins, W.G., 2000. Measures of reliability in sports medicine and science. Sports Med. 30, 1–15.
Huang, C.K., Kitaoka, H.B., An, K.N., Chao, E.Y., 1993. Biomechanical evaluation of longitudinal arch stability. Foot Ankle 14, 353–357.
Huerta, J.P., Garcia, J.M.A., 2007. Effect of gender, age and anthropometric variables on plantar fascia thickness at different locations in asymptomatic subjects. Eur. J. Radiol. 62, 449–453.
Kawakami, Y., Kanehisa, H., Fukunaga, T., 2008. The relationship between passive ankle plantar flexion joint torque and gastrocnemius muscle and achilles tendon stiffness: implications for flexibility. J. Orthop. Sports Phys. Ther. 38, 269–276.
Ker, R.F., Bennett, M.B., Bibby, S.R., Kester, R.C., Alexander, R.M., 1987. The spring in the arch of the human foot. Nature 325, 147–149.
Kumka, M., Bonar, J., 2012. Fascia_a morphological description and classification system based on aliterature review. J. Can. Chiropr. Assoc. 56, 179–191.
Lima, K., Costa Junior, J.F.S., Pereira, W.C.A., Oliveira, L.F., 2017. Assessment of the mechanical properties of the muscle-tendon unit by supersonic shear wave imaging elastography: a review. Ultrasonography 37, 3–15.
Ling, Y., Li, C., Feng, K., Duncan, R., Eisma, R., Huang, Z., Nabi, G., 2016. Effects of fixation and preservation on tissue elastic properties measured by quantitative optical coherence elastography (OCE). J. Biomech. 49, 1009–1015.
Ling, Z.X., Kumar, V.P., 2008. The myofascial compartments of the foot: a cadaver study. J. Bone Joint Surg. Br. 90, 1114–1118.
Moraes do Carmo, C.C., Fonseca de Almeida Melao, L.I., Valle de Lemos Weber, M.F., Trudell, D., Resnick, D., 2008. Anatomical features of plantar aponeurosis: cadaveric study using ultrasonography and magnetic resonance imaging. Skeletal Radiol. 37, 929–935.
Pavan, P.G., Pachera, P., Stecco, C., Natali, A.N., 2014. Constitutive modeling of time-dependent response of human plantar aponeurosis. Comput. Math. Methods Med. 2014, 530242.
Pavan, P.G., Stecco, C., Darwish, S., Natali, A.N., De Caro, R., 2011. Investigation of the mechanical properties of the plantar aponeurosis. Surg. Radiol. Anat. 33, 905–911.
Saavedra, A.C., Zvietcovich, F., Lavarello, R.J., Castaneda, B., 2017. Measurement of surface acoustic waves in high-frequency ultrasound: preliminary results. Conf. Proc. IEEE Eng. Med. Biol. Soc.
Scher, D.L., Belmont Jr., P.J., Bear, R., Mountcastle, S.B., Orr, J.D., Owens, B.D., 2009. The incidence of plantar fasciitis in the United States military. J. Bone Joint Surg. Am. 91, 2867–2872.
Stecco, C., Corradin, M., Macchi, V., Morra, A., Porzionato, A., Biz, C., De Caro, R., 2013. Plantar fascia anatomy and its relationship with Achilles tendon and paratenon. J. Anat. 223, 665–676.
Strickler, T., Malone, T., Garrett, W.E., 1990. The effects of passive warming on muscle injury. Am. J. Sports Med. 18, 141–145.
Thordarson, D.B., Schmotzer, H., Chon, J., Peters, J., 1995. Dynamic support of the human longitudinal arch. a biomechanical evaluation. Clin. Orthop. Relat. Res. 316, 165–172.
Uritani, D., Fukumoto, T., Matsumoto, D., Shima, M., 2014. Reference values for toe grip strength among Japanese adults aged 20–79 years: a cross-sectional study. J. Foot Ankle Res. 7, 28.
Werner, R.A., Gell, N., Hartigan, A., Wiggerman, N., Keyserling, W.M., 2010. Risk factors for plantar fasciitis among assembly plant workers. PM R. 2, 110–116.
Wilke, H.J., Werner, K., Haussler, K., Reinehr, M., Bockers, T.M., 2011. Thiel-fixation preserves the non-linear load-deformation characteristic of spinal motion segments, but increases their flexibility. J. Mech. Behav. Biomed. Mater. 4, 2133–2137.
Zelik, K.E., La Scaleia, V., Ivanenko, Y.P., Lacquaniti, F., 2015. Coordination of intrinsic and extrinsic foot muscles during walking. Eur. J. Appl. Physiol. 115, 691–701.
Zhang, L., Wan, W., Zhang, L., Xiao, H., Luo, Y., Fei, X., Zheng, Z., Tang, P., 2014. Assessment of plantar fasciitis using shear wave elastography. Nan Fang Yi Ke Da Xue Xue Bao 34, 206–209. in Chinese.